



Improving manganese circular economy from cellulose by chelation with siderophores immobilized to magnetic microbeads

Peter M. Kunz¹ · Kerstin Mörtter¹ · Ralf Müller² · Isabell Sommer¹ · Philipp Weller² · Jeff Wilkesman^{1,3}

Received: 5 February 2020 / Accepted: 26 August 2020 / Published online: 9 September 2020
© The Author(s) 2020

Abstract

Manganese (Mn) contained in cellulose is partially responsible for an increased consumption of paper bleaching chemicals (like O₂, H₂O₂), consequently diminishing the efficiency in pulp processing, darkening the pulp and deteriorating pulp quality. Usually, Mn in the paper industry is removed employing the environmentally critical EDTA. A greener alternative constitutes, however, the use of siderophores, high-affinity metal-chelating organic compounds that are produced by microorganisms to acquire metals (Fe and Mn among others), like desferrioxamine B (DFOB) or desferrioxamine E (DFOE). The use of native Mn-transporter proteins, like PrtA, constitutes another possibility for Mn removal. The evaluation of utilizing siderophores or PrtA for Mn removal from cellulose in a circular economy scheme is therefore essential. Firstly, Mn removal from cellulose was performed by immobilizing siderophores or PrtA on magnetic beads (M-PVA C22). Secondly, the beads were incubated overnight with a 2% cellulose suspension, allowing Mn-ligand complex formation. Finally, cellulose suspensions were submitted for Mn quantification, employing either the TCPP [Tetrakis(4-carboxyphenyl)porphyrin] method, the PAN [*l*-(2-pyridylazo)-2-naphthol] method or the Inductively Coupled Plasma-Optical Emission Spectroscopy (ICP-OES). When non-immobilized ligands were employed, a 31% Mn removal was achieved; when using immobilized ligands, around 10% Mn removal was obtained. Treated and untreated cellulose was analyzed by SEM and the Mn distribution between the solid and liquid phase was parameterized using adsorption isotherm models. This novel greener method proved to be feasible and easy, leading to potential improvements in the paper industry. Next research steps are to optimize Mn removal and quantify Mn recovery after ligand decoupling before scaling-up.

Keywords Circular economy · ICP-OES · Manganese · Siderophores

Electronic supplementary material The online version of this article (<https://doi.org/10.1007/s10668-020-00962-0>) contains supplementary material, which is available to authorized users.

✉ Jeff Wilkesman
j.wilkesman@lba.hs-mannheim.de

Extended author information available on the last page of the article

1 Introduction

Manganese (Mn) is among the main impurities that need to be removed from pulp. Peroxide treatment is generally present in modern bleaching sequences, needing a previous metal removal step from the pulp (viz. Mn, Fe and Cu). Mn(II) has a negative impact on the efficiency of bleaching with oxygen-based chemicals due to its decomposing effect through peroxide, worsening overall pulp quality and causing darkening of the pulp (Pinto et al. 2015). Removal of Mn adsorbed to the fiber phase is characteristically carried out at pH values between 4.5 and 6. At pH > 7, Mn(II) is chelated less effectively, and hence, its removal cannot be performed by dewatering and washing in subsequent steps in the pulp manufacturing. Between 14 and 50 mg Mn per kg of dry pulp can be extracted with almost complete removal of Mn at pH values as low as 5.5 and as high as 9.5 (Elofson and Nordgren 1996; Pinto et al. 2015).

Usually, a chelating treatment or an acid wash of the pulps is performed for metal removal (Granhölm et al. 2010b). Nonetheless, commonly employed chelating agents like EDTA (ethylenediaminetetraacetic acid) or DTPA (diethylenetriamine penta-acetic acid) are poorly biodegradable under the standard working conditions and are only partially eliminated in biological treatment plants. There is also a possibility to dose some of the chelating agent in the closed part of the mill and thus lower the emissions from the bleach plant. Between 25 and 40% of charged chelating agents have been identified in waste water analyses of market Kraft pulp mills, i.e., 10–15 mg EDTA L⁻¹ effluent, representing 2 kg EDTA per ton pulp (European Commission 2015).

Metal ion desorption from pulps by chelation with EDTA is a complex chemical process not fully understood. The removal process is basically governed by the strength of the metal–EDTA complex formed (log *K*), but also on how strong metal ions are bound to other functional groups present in the pulp. Sequestering agents are generally defined as those able to remove Mn ions (or any other metal) from the solution system by generally forming a ring where the metal ion forms complex bonds with the ligand. Besides EDTA, other typical agents used for Mn sequestration are polyphosphates, sodium silicate and humic acid. Table 1 summarizes some of the most common Mn chelators. Despite the widespread use of sequestering agents, research has not resulted in an effective method to directly evaluate the Mn complexation (Volpe 2012).

Granhölm et al. (2010a) stated that maximal removal of Mn from pulp was achieved with 0.025% EDTA for softwood pulps and 0.1% EDTA for hardwood pulps. EDTA and its related compounds are regarded as safe when used in cosmetic and pharmaceutical formulations; however, its facility in forming metal complexes, together with its environmental recalcitrance, brings as a consequence a major disconcertion of the natural metal speciation in the environment. When present in water, EDTA is able to solubilize heavy metals from soils and sediments, improving its mobility and consequently increasing the occurrence of metals in water supply systems (Pinto et al. 2013).

Given that heavy metal mobilization is enhanced by EDTA complexation (including also solubilization of radioactive metals), much attention has been raised concerning direct or indirect potential effects of EDTA in the environment. Currently, environmental problems arise not only from the toxicity of the EDTA, but mainly from the high stability of the complexes formed and its low tendency to adsorb, making EDTA removal from waste water difficult (European Commission 2015, Oviedo and Rodríguez 2003).

The European Union and Australia banned EDTA in detergents due to its recalcitrance and potential mobilization of heavy metals and radionuclides. EDTA in natural waters is

Table 1 Common manganese chelators with their association constant values (expressed as log *K*) for some typical Mn(II/III) ligands (0.1 M solution, 25 °C)

Ligand	Log <i>K</i>	Reference
DFOB [desferrioxamine B]	29.9	Duckworth and Sposito (2005b)
DTPA [diethylenetriamine penta-acetic acid]	15.2	Ye et al. (2012)
EDTA [ethylenediaminetetraacetic acid]	13.6 (Mn ²⁺) 24.9 (Mn ³⁺)	Tanaka et al. (1965)
EGTA [ethylene glycol-bis(aminoethylether)- <i>N,N,N',N'</i> -tetraacetic acid]	12.5	Frausto da Silva and Williams (1991)
MGDA [methylglycinediacetic acid]	8.4	Pinto et al. (2013)
ENDA [ethylenediamine diacetate]	8.0	Frausto da Silva and Williams (1991)
NTA [nitrilotriacetic acid]	7.3	Pinto et al. (2013)
TRIEN [triethylenetetramine]	6.0	Frausto da Silva and Williams (1991)
PDA [pyridine-2,6-dicarboxylic acid]	5.0	Pinto et al. (2015)
Citric acid	3.2	Klewicky and Morgan (1998)
EN [ethylenediamine]	2.0	Frausto da Silva and Williams (1991)

present at high levels partly due to its extensive usage in industrial cleaning to remove calcium deposits, in detergent as a sequestering agent, and in the pulp and paper industries to form complexes with metal ions for better bleaching (Zhang et al. 2007).

Considering that 2 kg EDTA is needed for 1 ton pulp treatment mentioned earlier, and considering also the 5 million tons of pulp produced in, e.g., Germany (FNR 2017; see also Discussion), we may foresee the presence of around 10,000 tons EDTA. Consequently, other chelating alternatives have been proposed. Hitherto, some substitutes for EDTA in the paper pulp industry studied are novel amino acid derivatives like ethylenediamine-*N,N'*-disuccinic acid (EDDS), iminodisuccinic acid (IDS), pyridine-2,6-dicarboxylic acid (PDA), methylglycinediacetic acid (MGDA) or siderophores [like desferrioxamine B (DFOB) or desferrioxamine E (DFOE)] (Hyvonen et al. 2006; Metsarinne et al. 2007; Pinto et al. 2015; Wilkesman et al. 2019).

DFOB, which is a linear trihydroxamic acid siderophore produced by bacteria, is known to act as a high affinity shuttle to sequester Fe(III) and Mn(III) from an inorganic or biological source and thus is attractive for metal ion sensing and remediation (Codd et al. 2018). The strong interaction between Mn(III) and DFOB promotes oxidation of the siderophore-chelated Mn(II) to Mn(III) and thus stabilizes the Mn(III) oxidation state. Furthermore, it has been suggested that this oxidation process plays a primary role in the biogeochemical cycle of Mn by manganese-oxidizing microorganisms (Farkas et al. 2014).

Although on the one hand EDDS, which combines chelation efficiency and biodegradability, seems to be a suitable alternative for EDTA, siderophores like DFOB, on the other hand, have the advantage of being commercially available biomolecules, are readily soluble, and show pH stability throughout a wide range (Duckworth and Sposito 2005a). Siderophores are indeed effective agents in pulp treatment, reducing up to 70% of the needed bleaching chemicals to Kraft pulp (Ahmed and Holmström 2014). Though siderophores are environment-friendly alternatives, further research regarding green and more efficient competitive chelating agents to be used in the paper pulp industry is awaiting.

The use of native Mn-transporter proteins may also represent an option for Mn removal. PrtA (processing-associated tetratricopeptide repeat protein) is a Mn transport protein (35 kDa) of the photosynthetic system and is proposed here, besides siderophores, as another possible way for Mn removal. PrtA isolated from the cyanobacterium *Synechocystis sp.* PCC6803 is required for efficient delivery of Mn(II) to the photosystem II in vivo (Stengel et al. 2012). In view of the high affinity binding site available in PrtA, which can only be occupied by Mn(II), a high selectivity in the complex formation is expected.

Here, a bionic inspired Mn complexation employing siderophores (DFOB, DFOE) and the protein PrtA in a cellulose pulp suspension is proposed and thus may contribute to the putative substitution of EDTA. The chelation of Mn proceeds employing ligands preimmobilized to the magnetic carrier (microparticles M-PVA C22). The Online Resource contains supplementary information with the complexation reaction between Mn and DFOB (Fig. S1). A scheme of the circular recovery procedure is shown in Fig. 1, and the importance and impact of Mn removal for the near future is highlighted in a brief circular economy analysis given ahead.

2 Materials and methods

2.1 Materials

The unbleached cellulose pulp, generated after a sulfate process, was provided by Zellstoff Stendal GmbH. Control cellulose, EDC, EDTA and MES were purchased from Sigma. Siderophores DFOB and DFOE were from ASA Spezialenzyme GmbH (Nr. 5020, Wolfenbüttel, Germany). The Mn determination kit (0.005–5 mg Mn/L; LCW 532) employing the PAN method and the Mn standard solution ($1000 \pm 10 \text{ mg Mn}^{2+} \text{ L}^{-1}$) was purchased from Hach (USA). TCPP [5, 10, 15, 20-tetrakis (4-carboxyphenyl) porphyrin] was purchased from PorphyChem SAS (Dijon, France). HPLC water, methanol, trifluoroacetic acid,

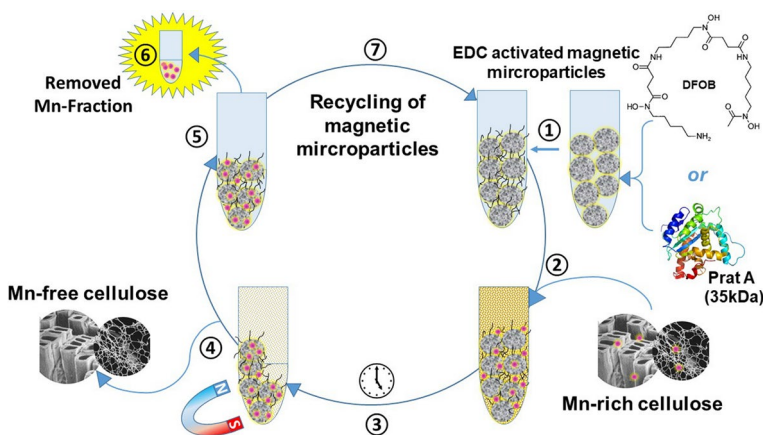


Fig. 1 Scheme for circular Mn removal. (1) Coupling of the cross-linker EDC-activated magnetic particles to PrtA or siderophore (DFOB). (2) Mixing of the microparticles with the Mn-rich pulp slurry. (3) Stirring and "fishing" the Mn complex. (4) Separation of the Mn carrier particles from the pulp slurry by magnetic separation. (5) Release of the manganese from the Mn carrier. (6) Concentration of the Mn fraction. (7) Recycling of the Mn-carrier particles

isopropanol were from Roth (Germany). Superparamagnetic magnetite particles (M-PVA C22 magnetite particles) were provided by Chemagen Technologies GmbH (CMG-207, PerkinElmer, Baesweiler, Germany). The magnet for the magnetite particles separation was a PureProteome™ Magnetic Stand, and the ICP-Multi-Element standard solution (IV) ($[\text{Mn}] = 994 \pm 10 \text{ mg/L}$; $[\text{Fe}] = 1000 \pm 10 \text{ mg/L}$) was from Merck (Germany). All other chemicals used were of high purity.

2.2 Pulp sample preparation

Samples were prepared as described by Pinto et al. (2015) with minor modifications. To proceed with the Mn removal present in the pulp, 2% (m/v) pulp suspensions were mixed with the aqueous complexing agents [50 mg mL^{-1} DFOB, 50 mg mL^{-1} DFOE or 1 mg mL^{-1} PratA (kindly provided by Prof. Dr. J. Nickelsen, LMU Munich); 0.01 mg mL^{-1} EDTA used as control] and incubated at $50 \text{ }^\circ\text{C}$ overnight. The suspensions were filtered, and metal concentration was analyzed. In order to study cellulose morphology, samples were fixed with Leit-C-Tab obtaining a 15-nm carbon coating and were subsequently examined by scanning electron microscopy performed on a Carl Zeiss Gemini 500 field emission SEM at an accelerating voltage of 5 kV with different magnifications.

2.3 Mn and Fe concentration determination

The cellulose suspensions were filtered, and the solids as well as the filtrates were kept, and the metal concentration determined in each fraction using an Optima 2000 DV ICP-OES system (PerkinElmer, λ 257,610, detection limit 0.03 ppb) similarly as that proposed by Zeiner et al. (2012). Each experiment was carried out in triplicate. In addition, the samples were tested using photometric methods. For this, the PAN [*l*-(2-pyridylazo) -2-naphthol] method (Hatat-Fraile and Barbeau 2019) and the TCPP [*l*-(5, 10, 15, 20-tetrakis (4-carboxyphenyl) porphyrin)] method were used. Control solutions of the complexes Mn(II/III)-DFOB or Mn(II/III)-DFOE were prepared similarly as reported by Madison et al. (2011). The pH was adjusted to 8.0, and the concentration of Mn-siderophore complex was determined using its absorbance peak at 310 nm ($\epsilon_{310} = 2062 \text{ M}^{-1} \text{ cm}^{-1}$) (Springer and Butler 2015). Diluted standard calibration solutions of Mn(II) were prepared by duplicate from a commercial multi-element standard solution at concentrations between 0.0010 and 10 mg L^{-1} (Mn^{2+} or Fe^{2+}), dissolved in Milli-Q ultrapure water without pH adjustment.

2.4 Immobilization

For the immobilization, superparamagnetic magnetite particles (M-PVA C22 magnetite particles) were used, which consist of a matrix made of polyvinyl alcohol and were correspondingly carboxylated on the surface for binding with PratA or siderophores. The functional groups are seated on a C22 spacer arm, and the particles have a polydisperse size distribution (\varnothing 1–3 μm). The immobilization was carried out in Eppendorf tubes, and the magnetite particles were separated using a magnet. First the magnetic particles were activated. For this, $\sim 7 \text{ mg}$ particles ($150 \mu\text{L}$ of the $50 \mu\text{g } \mu\text{L}^{-1}$ particle solution) were washed twice with 1 mL 0.1 M MES buffer pH 5.3. The particles were then activated with 1 mL EDC (*l*-ethyl-3-(3-dimethylaminopropyl)carbodiimide hydrochloride) solution (50 mg EDC in 1 mL MES) and incubated for 2 h in a shaker at $25 \text{ }^\circ\text{C}$. The particles were then

washed again three times with 1 mL MES buffer in order to completely remove the EDC residues (Ferner et al. 2018; Kazenwadel et al. 2015; Morhardt et al. 2014).

The ligands (DFOB, DFOE or Prata) were immobilized by incubating 100 μL protein solution or 1 mL saturated siderophore solution (50 mg mL^{-1}) in the corresponding buffer with 7 mg (150 μL) of the separated and activated particles while shaking for 18 h, 4 °C, in a shaker at 300 rpm. The particles were then washed twice with 1 mL MES buffer. The immobilized siderophores (or protein) were stored at 4 °C.

2.5 FTIR ATR spectroscopy and RP-HPLC

Samples containing the immobilized siderophore-Mn complex were further characterized by Fourier Transform Infrared Attenuated Total Reflection (FTIR ATR) spectroscopy and RP-HPLC (Anke et al. 2017; Edwards et al. 2005; Morhardt et al. 2014; Schwabe et al. 2018). A Bruker Optics Tensor 27 spectrometer (Ettlingen, Germany) with room temperature deuterated triglycine sulfate (RT-DTGS) detector and a Bruker Optics Platinum® ATR accessory (diamond crystal with one reflection) were applied. All spectra were recorded at 21 °C using the software Bruker OPUS 7.2. Spectra were recorded from 4000 to 400 cm^{-1} with a resolution of 4 cm^{-1} against an air background. All magnetic beads measured by FTIR ATR were separated from the supernatant and dried overnight at 60 °C.

Each sample was measured 10 times, and between measurements, the sample was moved on the crystal with a spatula to minimize the effect of the particle distribution in the measurement point of the ATR accessory. Between the samples, the crystal was cleaned using ethanol and the cleanliness of the crystal was validated with a measurement of the 100% line. After measurements, an atmospheric compensation for atmospheric water and aqueous solution was performed within OPUS.

For the RP-HPLC a Dionex system (Thermo Scientific) with a C18 guard-column and column (HyPURITY AQUASTAR, Thermo Scientific; 5 μm particles of 180 Å, 150 mm length, with 4.6 mm inner diameter) was employed. The elution was performed at 1 mL min^{-1} with 28% methanol and 72% deionized H_2O (supplemented with 0.1% trifluoroacetic acid). After the run, the column was washed with 95% methanol and equilibrated prior to the next separation. Five different wavelengths (217, 250, 274, 310 and 426 nm) were used for monitoring the Mn complex.

2.6 Adsorption isotherms

Mn desorption from cellulose was measured at pH 8.0. Approximately 0.20 g cellulose and 10 mL of a solution containing 75 mM imidazol buffer were added to a 50-mL falcon tube. The mixture was heated for 2 h at 70 °C and then was homogenized with an ultraturax for 10 min. DFOB was added to the suspension [final concentration 0–30 mM] and was left mixing in orbital motion overnight to guarantee equilibrium conditions. Afterward, the suspension was filtered (PVDF membrane 0.45 μm). The determination of DFOB or Mn at equilibrium concentration was done by taking an aliquot of 1 mL of the filtrate and diluting with water to a final volume of 11 mL. Adsorption control experiments were conducted without DFOB. Experiments were done in duplicate. The amount of Mn uptake by the ligand (DFOB) was calculated by mass balance relationship equation as follows (Pani et al. 2017; Thongpitak et al. 2019):

$$q_e = ([\text{Mn}]_o - [\text{Mn}]_{eq}) / [\text{cellulose}]$$

where $[\text{Mn}]_o$ and $[\text{Mn}]_{eq}$ are the initial and equilibrium concentrations of Mn ($\mu\text{mol/L}$) and the cellulose concentration is expressed in g/L . The equilibrium adsorption capacity, q_e , is expressed in mmol/kg . The linearization of the Langmuir relationship:

$$q_e = q_{\max} \cdot K_L [\text{Mn}]_{eq} / (1 + K_L \cdot [\text{Mn}]_{eq})$$

gives the expression:

$$1/q_e = 1/(q_{\max} \cdot K_L \cdot [\text{Mn}]_{eq}) + 1/q_{\max}$$

where q_{\max} and K_L are the Langmuir constants related to adsorption. Given that cellulose is considered a highly heterogeneous material, the Freundlich isotherm was also employed in the analysis:

$$q_e = K_F([\text{Mn}]_{eq})^{1/n}$$

where n and K_F are Freundlich isotherm constants. The linearization of the latter gives the expression:

$$\log q_e = \log K_F + (1/n) \log [\text{Mn}]_{eq}$$

Furthermore, the Hill equation was used to analyze the interaction of the ligand [L] with the metal [M] according to the equation:

$$\theta = [\text{ML}]/[\text{Mn}]_o = K_d[\text{L}]^n / (1 + K_d[\text{L}]^n)$$

This is expressed after linearization as:

$$\theta/[\text{L}]^n = ([\text{L}]^n/K_d) - (1/K_d)$$

where [ML] is the molar concentration of the metal–ligand (Mn-DFOB) complex, $[\text{M}]_o$ is the initial Mn concentration (μM) in the pulp, K_d is the dissociation constant, [L] is the ligand concentration (μM), and n is the Hill coefficient.

3 Results and discussion

3.1 Determination of Mn and Fe concentration

As indicated by scanning electron microscopy (SEM), the cellulose samples with or without treatment retained its fibrous morphology, compared to control samples (Fig. 2). Retention of this fibrous nature can be considered as an important characteristic as the treatment did not affect the morphology of the sample and thus its characteristics for the ultimate purpose in the pulp industry are maintained.

Mn quantification was approached by three different methods. The Mn assay kit was used only for filtrates, as not completely homogeneous samples containing partially solubilized cellulose caused interference with the absorbance reading. In the case of the TCP method, the Mn concentration of some samples was below the detection limit ($10 \mu\text{g L}^{-1}$) (Hatat-Fraile and Barbeau 2019). The most reliable determination of the Mn concentration was performed using ICP-OES. The calibration curve of Mn^{2+} and

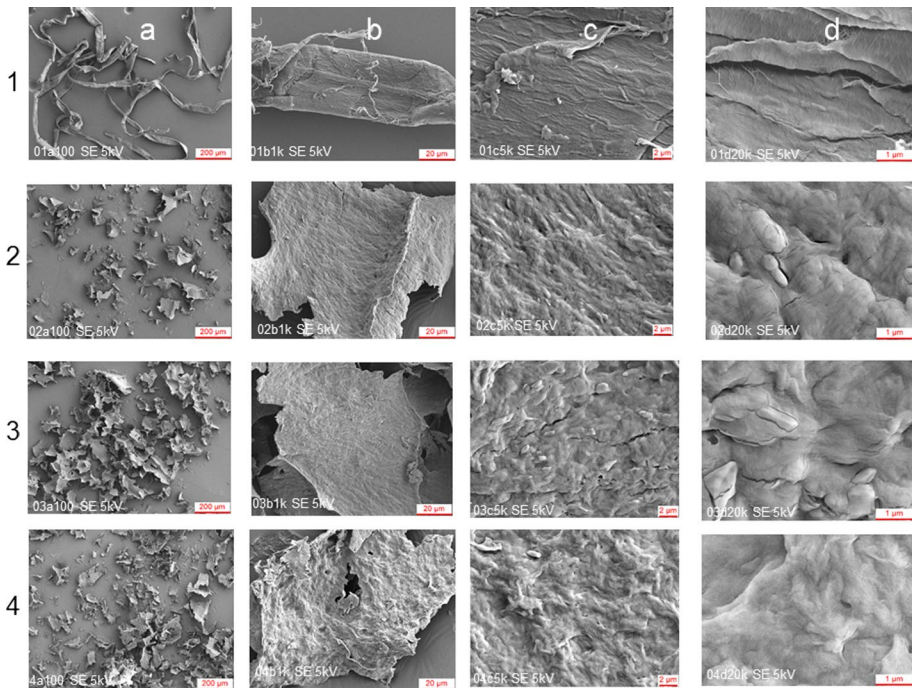


Fig. 2 SEM images of the different cellulose samples. Row (1) shows the original raw cellulose without homogenization procedure, (2) cellulose treated for Mn removal with DFOB immobilized to magnetic beads, (3) cellulose treated without DFOB but submitted to magnetic beads and (4) control homogenized cellulose. Columns show the different resolutions: **a** 200, **b** 20, **c** 2 and **d** 1 μm

Fe^{2+} is presented in Online Resource (Fig. S2). Dry cellulose was analyzed for determination of initial total metal concentration. Per kg of dry cellulose, 14.5 ± 0.7 mg Mn was determined via ICP-OES, with an iron content of 6 ± 4 mg Fe per kg of dry cellulose, similar to previously reported values (Kujala et al. 2004; Pinto et al. 2015). The Mn and Fe content from the dry cellulose and pulp suspension samples was measured via ICP-OES, and results are shown in Tables 2 and 3, respectively. The chelating process proceeds via the formation of a complex with a log K of 29.9 (Table 1) (Online Resource, Fig. S1). This metal sequestration by siderophores may be considered a desorption process and was thus calculated as follows (Tian et al. 2019):

$$\%(\text{Mn})_{\text{removed}} = 100 \cdot ([\text{Mn}]_o - [\text{Mn}]_t) / (V/m)$$

Table 2 Initial metal content in dry cellulose

Metal	mg metal / kg dry cellulose	mmol metal / kg dry cellulose	2% (m/v) Concentration ($\mu\text{mol L}^{-1}$)
Mn	14.5 ± 0.7	0.26	5.3
Fe	6 ± 4	0.11	2.1

Table 3 Metal quantification via ICP-OES

Chelator	Metal concentration		Metal removal	
	(mg kg ⁻¹)		(%)	
	Mn (±0.7)	Fe (±4)	Mn (±2)	Fe (±2)
None	27.8	46	–	–
0.01 mg mL ⁻¹ EDTA	18.2	17	35	63
50 mg mL ⁻¹ DFOB	19.1	14	31	69
1 mg mL ⁻¹ Prata	27.7	21	0.2	54

The pulp suspensions were pretreated (50 °C, overnight, pH 9.0). Metal removal is given as a percentage after 24-h treatment with an excess of chelator. Standard deviation (±) given from triplicates

where $[Mn]_o$ is the manganese concentration in pulp without treatment (control sample treated without chelator) (mg/L), $[Mn]_t$ is the manganese concentration in pulp after chelator treatment at the given specific incubation time (mg/L), V is the volume (L) of the solution, and m is the mass (kg) of pulp.

The samples were treated with the different chelators. Metal removal from the pulp with EDTA and DFOB gave similar values (on average 33% Mn and 66% Fe removed). Prata was unable to couple Mn under the chosen experimental conditions.

3.2 Adsorption isotherms

To further analyze the Mn sequestration process, adsorption isotherms were constructed varying the concentration of DFOB (0–30 mM). Figure 3 and Table 4 show the results of the adsorption experiments. The isotherms indicate the distribution of the Mn between the liquid and solid phases when the desorption process extends to a state of equilibrium. The most frequently isotherm models employed to determine the equilibrium of adsorption systems are the Langmuir and Freundlich isotherm models. The Hill equation was also employed to analyze the interaction between the metal and the ligand. Results show a better correspondence to the Freundlich model (Fig. 3c). Three essential premises of the Langmuir isotherm are monolayer coverage, adsorption site equivalence and independence; however, in solution systems, the adsorption of solutes on solid surface is not necessarily valid. Surface heterogeneity directly influences adsorption, thus deviating from the Langmuir premises. Though results show a fair linear tendency of the Langmuir model, care must be taken with the values obtained, and further analysis is visualized. The Freundlich model adapts better to the data, giving a higher value for the correlation coefficient, R^2 . The model assumes that adsorption occurs on a heterogeneous surface due to the diversity of the adsorption sites or the diverse nature of the metal ion adsorbed (Pani et al. 2017; Sohn and Kim 2005).

3.3 Siderophore immobilization

Table 5 shows the calculated concentration of bound Mn during immobilization on M-PVA C22 magnetic beads with the different chelators. From the values it can be concluded that DFOE acted as the strongest Mn remover (15%), with DFOB and Prata achieving similar but lesser values (lower than 10%). Iron concentration could not be

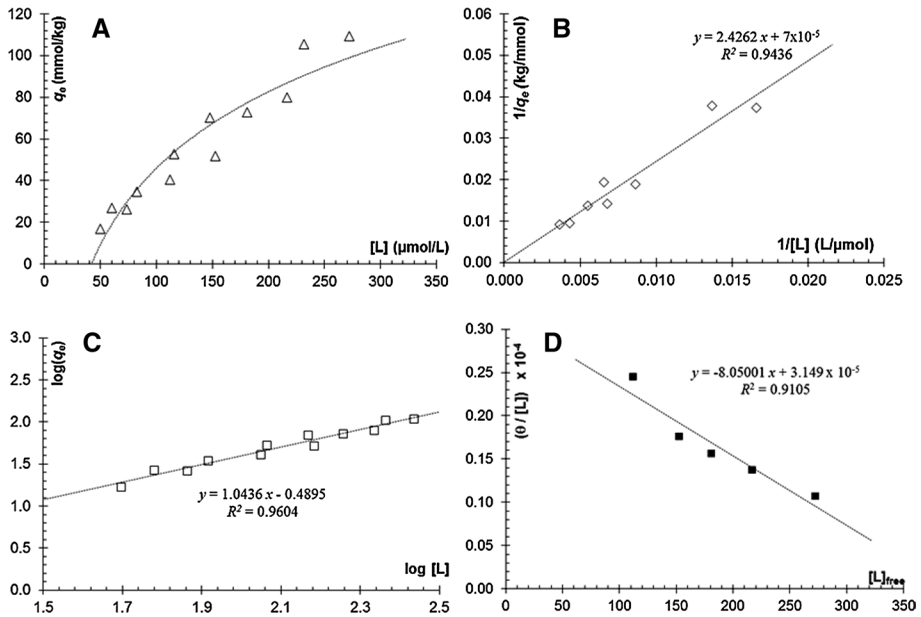


Fig. 3 Adsorption isotherms analysis. **a** Adsorption capacity (q_e in mmol kg^{-1}) versus free DFOB (μM). **b** Parameterized Langmuir isotherm model. **c** Parameterized Freundlich isotherm model and **d** the Hill representation. Unless otherwise stated, conditions were 20 g L^{-1} cellulose, 75 mM imidazol buffer pH 7.9, at 25°C . Equilibrium conditions were reached after 18-h incubation. All assays were performed by duplicate. Error bars have been omitted for better visualization of the data

Table 4 Adsorption model constants determination

Model	Parameters		
Langmuir	q_{max}	K_L	R^2
	13,489 (mmol g^{-1})	5560 (mM^{-1})	0.9436
Freundlich	$(1/n)$	K_F	R^2
	1.04	0.324 (mM^{-1})	0.9604
Hill	n	K_d	R^2
	1	31,760	0.9105

determined in this study due to the Fe content of the magnetite particles. For this determination, the PAN method was performed. To determine the total Mn concentration present in the cellulose suspension used for the immobilization, a sample was taken previous to the immobilization, giving a reference value of 5.9 mg Mn L^{-1} .

The magnetic beads, previously activated with EDC, were incubated with the chelators and then further incubated with the cellulose suspension. For the spectrophotometric reading, $500 \mu\text{L}$ was diluted in water to a final volume of 10 mL . As control, a sample containing no chelators was used. With this method, the non-bound Mn was measured. The amount of bound Mn was obtained by subtracting the Mn concentration of the sample from the total Mn concentration present in the cellulose suspension. The bound Mn concentration was divided by the total Mn concentration present in the

Table 5 Concentration of bound Mn after immobilization assay determined with the PAN method

Sample composition	Bound Mn (mg L ⁻¹)	Bound Mn (%)	Bound Mn (normalized) (%)
EDC-magnetic particles + cellulose suspension	2.7 ± 0.2	47 ± 3	0 ± 3
EDC-magnetic particles + cellulose suspension + DFOB	3.3 ± 0.2	56 ± 3	9 ± 3
EDC-magnetic particles + cellulose suspension + DFOE	3.6 ± 0.4	62 ± 6	15 ± 6
EDC-magnetic particles + cellulose suspension + Prata	3.2 ± 0.1	54.1 ± 0.2	7.1 ± 0.2
Cellulose suspension without immobilization procedure	5.9 ± 0.1	–	–

Percentage of Mn removal was calculated for each chelator. Standard deviation (±) given from triplicates

cellulose suspension to obtain the percentage of bound Mn to the complex. Using the control without chelator, the percentage was normalized.

The use of M-PVA C22 magnetic beads has the advantage of enabling the direct immobilization of the ligand on the magnetic particle, being possible at a later stage to easily remove the Mn-ligand complex from the cellulose with a magnet. Nevertheless, one must consider also that the PVA molecular chain contains a large number of hydroxyl groups, which could assuredly adsorb metal ions by hydrogen bonding and cross-linking (Tian et al. 2019). M-PVA C22 magnetic beads have a carboxyl functionalization with an amount of 900 μmol COOH/g bead, according to the manufacturer. However, information regarding the degree of hydrolysis or the degree of polymerization is not given by the provider and these parameters were consequently not evaluated in our studies, and still they do remain critical for the performance of PVA (Guo et al. 2018). It must be stated that PVA was not a variable considered in our study, as it was taken as an independent and constant component attached to the commercial magnetic beads. It is indeed important to take into account possible interactions of PVA with metal ions; however, this would represent a different research goal belonging to another project that we would certainly be willing to develop ahead.

To verify the results and for an extended characterization, the samples were prepared for Fourier Transform Infrared Attenuated Total Reflection (FTIR ATR) spectroscopy (Fig. 4) and the immobilization analysis complemented by RP-HPLC (Fig. 5). For the FTIR ATR spectra of the different samples analyzed (Fig. 4 A-F), focus was placed on the previously reported band assignments by Morhardt et al. (2014). There were different types of changes according to the sample, but in general the regions with the biggest change were the amide regions (1542, 1652 cm⁻¹). Still, more analyses must be performed as there are still many variations among samples and band assignment proved to be not simple.

The detection of Mn-loaded siderophore complexes via RP-HPLC (Fig. 5a) gave similar results as published by Anke et al. (2017). However, this is the first time that the elution profile for DFOE is presented. The elution time for the Mn-DFOE peak was 9.5 min, and the maximum absorption was determined to coincide with the Mn-DFOB complex (Fig. 5b). It must be stated, however, that complex formation is highly pH dependent, registering absorbance variation in the range from pH 4 to 9 (Fig. 5c).

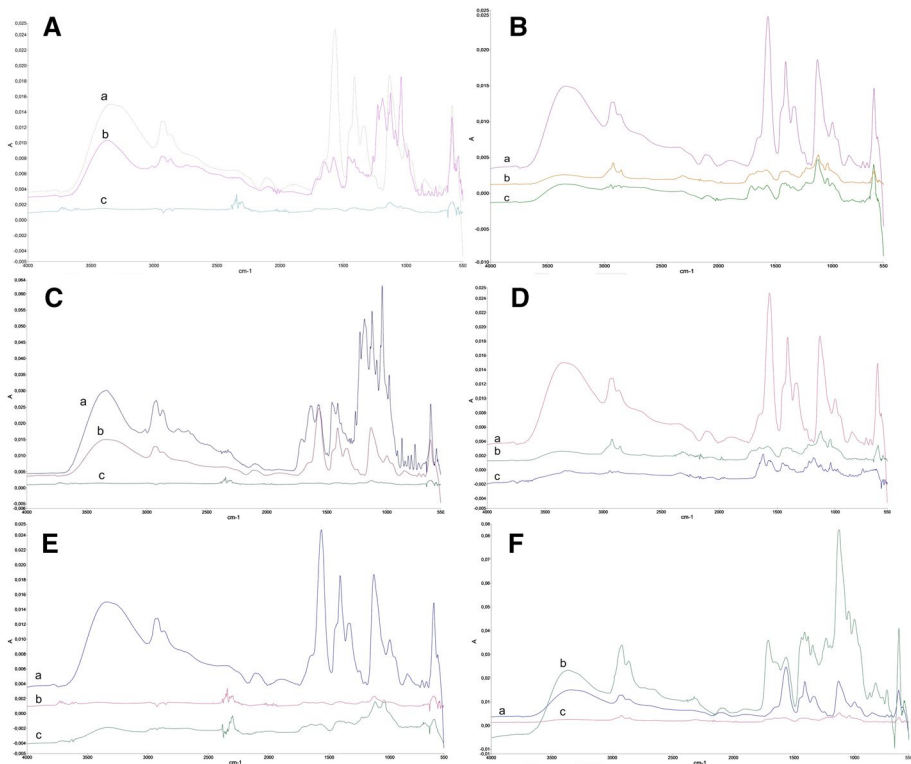


Fig. 4 Representative examples of FTIR ATR spectra of magnetic beads with or without covalently immobilized Mn-ligand complex. For all cases (A–F), spectrum (a) corresponds to PVA C22 alone (control); spectrum (b) corresponds to magnetic beads with covalently immobilized Mn-ligand complex and spectrum (c) without the ligand (negative control). Spectrum (b) always contains PVA C22 and EDC plus one of the following for each case: (A) DFOB and cellulose, (B) DFOB and filtrate, (C) DFOE and cellulose, (D) DFOE and filtrate, (E) PratA and cellulose and (F) PratA and filtrate

Above pH 10 a brownish Mn precipitate forms, likely corresponding to Mn hydroxide forms $[\text{Mn}(\text{OH})^+]$ or $[\text{Mn}(\text{OH})_3^-]$, as proposed by Wang and Giammar (2015). Analogous results have been published in the analysis of DFOB and DFOE to selectively complex Ga^{3+} in wastewaters (Jain et al. 2019).

3.4 PratA complexation

Though Mn is an essential micronutrient, increased amounts are harmful to the organism and consequently only a specific narrow concentration range exists for beneficial effects. A specific protein mechanism must thus exist to carefully maintain Mn homeostasis. How Mn is distributed to the different compartments inside the cell (of cyanobacteria) is still not fully understood. Few proteins have been identified as hypothetical Mn transporter in the cyanobacterial model strain *Synechocystis sp.* PCC 6803 (Brandenburg et al. 2017; Eisenhut et al. 2018). The assembly factor PratA from *Synechocystis sp.* PCC 6803A has been found to bind a maximum of eight Mn^{2+} ions. The presence of multiple sites for Mn^{2+} binding has indicated the existence of a high-affinity Mn^{2+} binding site (K_d $73 \pm 31 \mu\text{M}$)

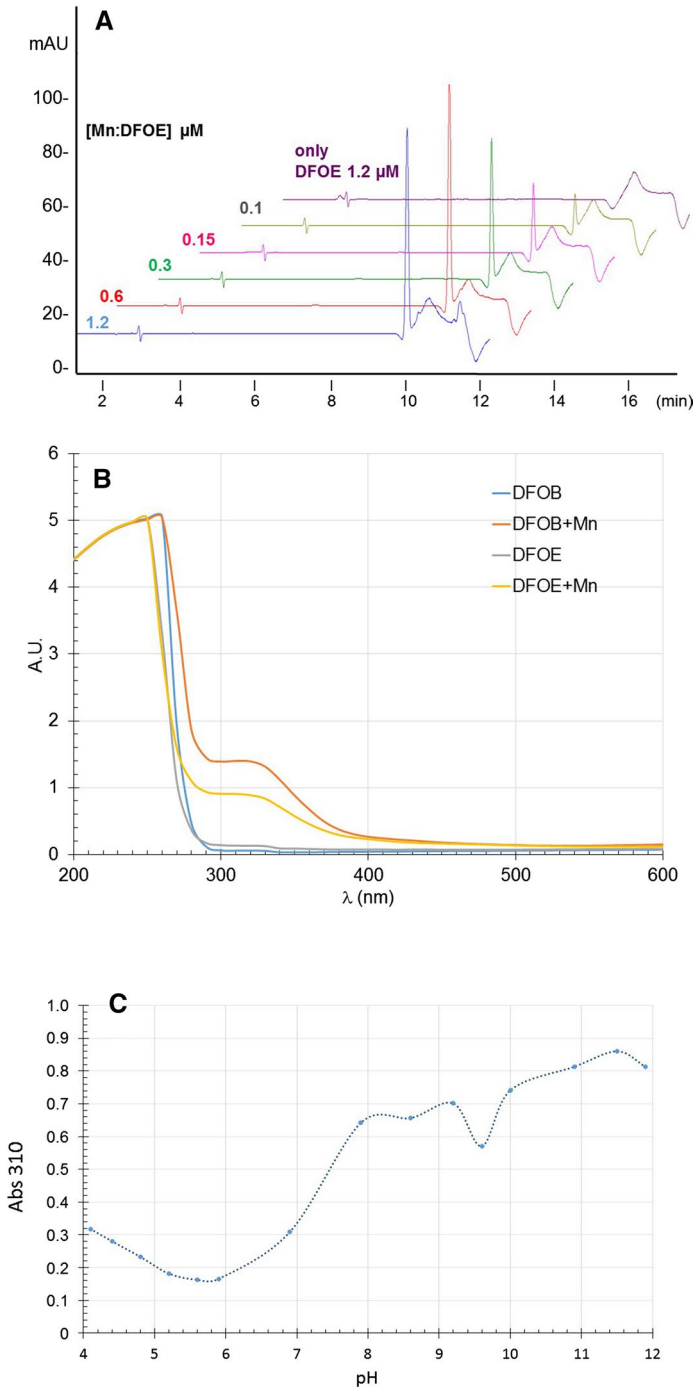


Fig. 5 Mn binding properties of DFOE analyzed by RP-HPLC. **a** The Mn-DFOE complex was prepared at different concentrations (1.2–0.1 μM) and eluted according to the RP-HPLC protocol with detection at 310 nm. **b** UV spectra of siderophores with and without Mn. **c** Dependence of the absorbance at 310 nm versus pH. A brown Mn precipitate forms after pH 10 is reached

and multiple low-affinity sites ($Kd_2 > 1$ mM) (Stengel et al. 2012). Fe^{3+} , Ca^{2+} and Mg^{2+} ions seem not to compete with Mn binding. Accordingly, it was proposed to employ PrataA as potential Mn chelator. Nevertheless, in first approaches, Mn concentration remained unchanged in the pulp sample treated with PrataA (Table 3). It is obvious that treatment at temperature over 40 °C and overnight must have led to protein denaturation.

In a second approach, PrataA was immobilized to the magnetic particles as shown in Fig. 1. With this method, it was possible to quantify a 7% Mn bound to immobilized PrataA, similar to DFOB and half as much as when using DFOE (Table 5). Unfortunately, due to the lack of more protein, further experiments were not performed.

3.5 Circular economy considerations

Industrial processes must meet extra requirements to achieve circular economy success. The closed-looped, energy-efficient and sustainable resource recovery processes must be compatible with health and environmental regulations, without losing financial profit. Therefore, an optimal environmentally friendly sustainable management can be achieved when appropriate raw materials are identified, clean production procedures are used, less waste is generated, materials are recycled, occupational exposure is controlled, and representative environmental data are collected. Zittel (2012) has reported that Mn may experience a peak production within the next 20 years, so concern should be raised regarding the proposal of a circular economy scheme for the proper use of Mn in new industrial methods. The use of Mn in OECD countries has been quantified to be in the order of 0.1 tons/person per year [Bermejo (2014), which is rather low compared to other metals] Fe 7–14; Al 0.35–0.5 tons/person per year. Still, the increasing use of Mn in the production of raw steel and upgrading ferroalloys, animal feed, dye for bricks, plant fertilizer components and dry-cell batteries, highlights the importance of conceiving a well-designed circular plan for its economy (Hagelstein 2009).

An interesting target for circular economy might be the water industry. Given that Mn(III) serves both as an oxidant and a reductant, and is considered a strong oxidant for one electron transfer reactions, Mn(III) would thus play a relevant role in water/wastewater treatment processes. It has been shown by Hu et al. (2017) that soluble Mn(III) efficiently degrades organics either through a non-oxidative or an oxidative pathway, depending on organic structural characteristics and functional groups present. According to Kohl and Medlar (2006), the major Mn removal treatment is oxidation with $KMnO_4$, followed by the use of pressure filtration systems and the use of an induced oxide-coated media. Reported was that only 1% of the water facilities studied uses sequestration. And yet, as stated by Tobiason et al. (2016), aesthetic problems rising from unexpected Mn(II) oxidation are solved through sequestration of Mn^{2+} by addition of polyphosphate or silicate, essentially for economic reasons.

Disappointingly, Mn(II) oxidation and precipitation occur within distribution system timescales, and in the presence of chlorine residuals in water distribution systems, as well as pipe wall biofilms; per se, sequestration may not seem to be as effective as originally thought. Effectiveness of the complex formation depends strongly upon the presence of other divalent cations (e.g., Fe^{2+} , Zn^{2+}), water hardness and its chemical stability. Hence, precipitated Mn particles are indeed an aesthetic problem and the particulate Mn may bear other concomitant elements such as arsenic or lead, which are extreme health concerns. Furthermore, the water industry could save significant costs and resources in decreasing

discoloration issues at the customer's tap by further researching the implications of the Mn(II/III) relation in order to improve removal of dissolved Mn (Johnson et al. 2018).

Astonishingly, rigorous health-based standards for Mn in drinking water are lacking (Tobiason et al. 2016). So far, during the design within integrated water treatment facility, Mn control is not considered properly, leading to doubtful water quality, at least under an aesthetic point of view. Successful Mn removal by treatment facilities is feasible if raw water quality is analytically characterized and if Mn physicochemical characteristics are considered.

Potential biotechnological applications exist also for biogenic manganese oxides. For example, disordered oxide structures (with defects and cation vacancies) can act as depolarizers in electrochemical cells. Now, the high affinity of biogenic manganese oxides for binding metals may propel them to be used for the bioremediation of metal contamination in waters and wastewaters (Wright et al. 2016). Manganese oxides have been also described as a good Lewis acid to modify contact-active surfaces, having an antimicrobial effect. The metal oxide serves as catalyzer for the chemical reaction of water into H_3O^+ , resulting in the damage of the microbial cell surface, destabilization of the pH gradient in the cell, as well as a negative influence on the overall enzyme activity and transport system, leading altogether ultimately to denaturation (Heimes et al. 2017).

Another example of the importance of Mn was the creation of a Manganese Research Cluster in 2015 by the German Federal Ministry of Education and Research, to determine the technological potential of manganese as a catalyst for electrolysis (FONA 2019). Clearly, Mn plays an extremely important role in the global economy, providing important socio-economic benefits in the regional context. Mn is directly and indirectly vital for our daily lives, either in the biochemical or industrial field. This scope includes materials in construction, manufacturing, agriculture, geobiochemistry, environmental, health and many others. Developing Mn applications (such as a cement additive, as batteries for electric vehicles, even as advanced high strength steels) reinforces future socio-economic and environmental benefits, according to Clarke and Upson (2017).

Worldwide Mn ore production (high grade containing over 40% Mn) is about 18.5 million tons per year (NS Energy 2020), while the production of manganese alloys is about 8 million tons per year. Primarily used in steelmaking, four families of manganese alloys are found: silicomanganese, high-carbon ferromanganese, medium- and low-carbon ferromanganese and manganese metal (Roskill Metals and Minerals Reports 2019). All manganese is consumed by the industries supplying the world, including construction (23%), engineering (14%) and transportation (11%). Manganese is recycled from iron and steel scrap, and a small amount is also recovered from used aluminum beverage cans. The recycling rate is 37%, and the efficiency of the whole recycling process is estimated to be 53% (Hagelstein 2009).

In general, a value as low as 0.4 mg Mn per kg pulp can be found. If one considers that, for example, in Germany alone in 2017 more than 5 million tons of pulp was consumed (FNR 2017), this would have corresponded to two tons of Mn that could have been recovered. It has been published (Bermejo 2014) that on average, each person consumes 0.1 ton Mn annually. Doing the math, the around 81 million inhabitants in Germany would thus consume approx. 8 million tons Mn. The use of Mn in the production of steel, ferroalloys, animal feed, dyes, fertilizers and batteries is constantly increasing, and the proposal of a good circular economy plan for Mn is thus important. Government and stakeholders need to recognize the relevance of Mn and support the need for

research for sustainable Mn production, meeting the needs of a modern and conscious society for the long term.

4 Conclusions

The immobilization of siderophores onto magnetic carriers and its use for chelating Mn present in cellulose suspensions was feasible. The use of siderophores is a major advance in employing greener methods for Mn removal. EDTA is typically used to separate Mn from the pulp; however, EDTA is the major organic pollutant in surface waters. Complete replacement of EDTA as a metal chelator in the paper industry is promptly needed, and siderophores (DFOB or DFOE) represent a viable and environmentally friendly alternative. The Mn content of pulp was determined by means of ICP-OES to be 15 mg Mn kg⁻¹ of dry cellulose. Isotherm adsorption analysis reveals a higher congruency with the Freundlich model, with a correlation factor of $R^2=0.9604$. A decrease between 7 and 15% in the Mn content from the cellulose suspension was determined. Mn immobilization values may be allegedly altered, given a recent personal communication from the manufacturer, confirming unreproducible Mn traces in the magnetic beads not formerly reported. The decoupling of Mn from the complex is still pending, nonetheless the process is environmentally friendly, and the results suggest that the use of immobilized siderophores can certainly improve metal removal and recycling in the paper industry. The assessment of sustainability (in terms of cost and performance parameters) needs to be further examined. Additional research regarding the formation of Mn complexes and the removal of Mn (II/III) will undoubtedly help the water and paper industry to develop better methods for optimizing the paper bleaching process and ultimately save considerable operating costs.

Acknowledgements This research was supported by the Baden-Württemberg Ministry of Science, Research and Art (Ideenwettbewerb Biotechnologie –Von der Natur lernen 7533-7-11.10-20). The authors kindly thank the collaboration of U. Heinemeyer and S. Becker for SEM analysis (BASF). The Alexander von Humboldt Foundation supported the stay of J. Wilkesman as a Philipp-Schwartz-Initiative Fellow. Special thanks go to J. Clear, C. Koch, A. Tomsche, L. Spiegel, S. Schilling and L. Kurz (Mannheim University of Applied Sciences), A. Werner (TU Dresden), E. Schneidenwind (Justus Liebig University Gießen), J. Nickelsen (LMU Munich), A. Cordes (ASA Spezialenzyme GmbH) and Zellstoff Stendal GmbH.

Author contributions All authors contributed to the study conception and revision. Peter M. Kunz and Isabell Sommer performed the theoretical and experimental conception and design of the work. Kerstin Mörtter was responsible for the experimental procedure, sample preparation, acquisition, analysis and interpretation of data. Ralf Müller, Philipp Weller and Jeff Wilkesman designed and performed the RP-HPLC, FTIR and ICP-OES analysis. Jeff Wilkesman validated results and elaborated the discussion. All authors read and approved the final manuscript.

Funding This study was funded by Baden-Württemberg Ministry of Science, Research and Art (Ideenwettbewerb Biotechnologie –Von der Natur lernen 7533-7-11.10-20), Huber Foundation (Nr. 1771990001954) and Alexander von Humboldt Foundation, Philipp-Schwartz-Initiative Fellowship. Open Access funding provided by Projekt DEAL.

Compliance with ethical standards

Conflicts of interest The authors declare no conflict of interest related to the publication of this paper.

Ethics approval Not applicable.

Consent to participate Not applicable.

Consent for publication The authors declare their consent for publication in this journal.

Availability of data and material (data transparency) Not applicable.

Code availability (software application or custom code) Not applicable.

Open Access This article is licensed under a Creative Commons Attribution 4.0 International License, which permits use, sharing, adaptation, distribution and reproduction in any medium or format, as long as you give appropriate credit to the original author(s) and the source, provide a link to the Creative Commons licence, and indicate if changes were made. The images or other third party material in this article are included in the article's Creative Commons licence, unless indicated otherwise in a credit line to the material. If material is not included in the article's Creative Commons licence and your intended use is not permitted by statutory regulation or exceeds the permitted use, you will need to obtain permission directly from the copyright holder. To view a copy of this licence, visit <http://creativecommons.org/licenses/by/4.0/>.

References

- Ahmed, E., & Holmström, S. J. M. (2014). Siderophores in environmental research: roles and applications. *Microbial Biotechnology*, 7, 196–208.
- Anke, M. K., Szymańska, K., Schwabe, R., Wiche, O., & Tischler, D. (2017). On the immobilization of desferrioxamine-like siderophores for selective metal binding. *Solid State Phenomena*, 262, 517–520.
- Bermejo, R. (2014). Circular economy: materials scarcity, European Union Policy and Foundations of a Circular Economy. In: Handbook for a Sustainable Economy. Dordrecht, Springer. https://doi.org/10.1007/978-94-017-8981-3_16. Accessed 19 July 2020.
- Brandenburg, F., Schoffman, H., Kurz, S., Krämer, U., Keren, N., Weber, A. P., et al. (2017). The synechocystis manganese exporter Mnx is essential for Manganese homeostasis in Cyanobacteria. *Plant Physiology*, 173, 1798–1810.
- Clarke, C., & Upson, S. (2017). A global portrait of the manganese industry—a socioeconomic perspective. *Neurotoxicology*, 58, 173–179.
- Codd, R., Richardson-Sanchez, T., Telfer, T., & Gotsbacher, M. (2018). Advances in the chemical biology of desferrioxamine B. *ACS Chemical Biology*, 13, 11–25.
- Duckworth, O., & Sposito, G. (2005a). Siderophore-manganese(III) interactions. I. Air-oxidation of manganese(II) promoted by desferrioxamine B. *Environmental Science and Technology*, 39, 6037–6044.
- Duckworth, O., & Sposito, G. (2005b). Siderophore-manganese (III) interactions II. Manganite dissolution promoted by desferrioxamine B. *Environmental Science and Technology*, 39, 6045–6051.
- Edwards, D. C., Nielsen, S. B., Jarzecki, A. A., Spiro, T. G., & Myneni, S. C. B. (2005). Experimental and theoretical vibrational spectroscopy studies of aceto-hydroxamic acid and desferrioxamine B in aqueous solution: effects of pH and iron complexation. *Geochimica Cosmochimica Acta*, 69, 3237–3248.
- Eisenhut, M., Hoecker, N., Schmidt, S. B., Basgaran, R. M., Flachbart, S., Jahns, P., et al. (2018). The plastid envelope CHLOROPLAST MANGANESE TRANSPORTER1 is essential for manganese homeostasis in *Arabidopsis*. *Molecular Plant*, 11, 955–969.
- Elofson, A., & Nordgren, A. (1996). Process for high-pH metal ion chelation in pulps. Patent No., 5,571,378.
- European Commission. (2015). Best available techniques (BAT) reference document for the production of pulp, paper and board. Institute for Prospective Technological Studies https://eippcb.jrc.ec.europa.eu/reference/BREF/PP_revised_BREF_042015.pdf. Accessed 19 July 2020.
- Farkas, E., Szabó, O., Parajdi-Losonczy, P., Balla, G., & Pócsi, I. (2014). Mn(II)/Mn(III) and Fe(III) binding capability of two *Aspergillus fumigatus* siderophores, desferriochelin and N', N'', N'''-triacetylfulsarine C. *Journal of Inorganic Biochemistry*, 139, 30–37.
- Ferner, M. J., Müller, G., Schumann, C., Shaikh, Y., Kampeis, P., Ulber, R., et al. (2018). Immobilisation of glycosidases from commercial preparation on magnetic beads. Part 2: Aroma enhancement in wine using immobilised glycosidases. *Vitis*, 57, 129–136.
- FNR, Fachagentur Nachwachsende Rohstoffe e. V. (2017). Verbrauch von Zellstoff in Deutschland 2017. <https://mediathek.fnr.de/grafiken/daten-und-fakten/biobasierte-produkte/papier-und-karton/verbrauch-von-zellstoff-in-deutschland.html>. Accessed 19 July 2020.

- FONA, Forschung für Nachhaltige Entwicklung. (2019). Funding for the MANGAN cluster project—manganese as a catalyst for electrolysis. <https://www.fona.de/en/mangan-cluster-project-manganese-as-a-catalyst-for-electrolysis-21941.html>. Accessed 19 July 2020.
- Frausto da Silva, J. J. R., & Williams, R. J. P. (1991). The biological chemistry of the elements, the inorganic chemistry of life, Ch. 14 (370–387). UK: Clarendon Press.
- Granhölm, K., Harju, L., & Ivaska, A. (2010a). Desorption of metal ions from kraft pulps. Part 1. Chelation of hardwood and softwood kraft pulp with EDTA. *BioResources*, 5(1), 206–226.
- Granhölm, K., Harju, L., & Ivaska, A. (2010b). Desorption of metal ions from kraft pulps. Part 2. Chelation of kraft pulps with different complexing agents and with EDTA in a reducing environment. *BioResources*, 5(4), 227–243.
- Guo, G., Xiang, A., & Tian, H. (2018). Thermal and mechanical properties of eco-friendly poly(vinyl alcohol) films with surface treated bagasse fibers. *Journal of Polymers and the Environment*, 26, 3949–3956.
- Hagelstein, K. (2009). Globally sustainable manganese metal production and use. *Journal of Environmental Management*, 90, 3736–3740.
- Hatat-Fraile, M., & Barbeau, B. (2019). Performance of colorimetric methods for the analysis of low levels of manganese in water. *Talanta*, 194, 786–794.
- Heimes, D., Kunz, P. M., Schilling, S., & Sommer, I. (2017). Antiadhäsive, antimikrobielle und kontaktaktive Oberflächen- unter dem Aspekt der unterschiedlichen Wirkprinzipien auf die Ansiedlung von Mikroorganismen und der Biofilm (Teil 2). *Galvanotechnik*, 11(108), 2312–2327.
- Hu, E., Zhang, Y., Wu, S., Wu, J., Liang, L., & He, F. (2017). Role of dissolved Mn(III) in transformation of organic contaminants: non-oxidative versus oxidative mechanisms. *Water Research*, 111, 234–243.
- Hyyonen, H., Orama, M., Arvelac, R., Henriksson, K., Saarinen, H., Aksela, R., et al. (2006). Studies on three new environmentally friendly chelating ligands. *Appita Journal*, 59, 142–149.
- Jain, R., Fan, S., Kaden, P., Tsumishima, S., Foerstendorf, H., Barthen, R., et al. (2019). Recovery of gallium from wafer fabrication industry wastewaters by Desferrioxamine B and E using reversed-phase chromatography approach. *Water Research*, 158, 203–212.
- Johnson, K., McCann, C., Wilkinson, J., Jones, M., Tebo, B., West, M., et al. (2018). Dissolved Mn(III) in water treatment works: Prevalence and significance. *Water Research*, 140, 181–190.
- Kazenwadel, F., Wagner, H., Rapp, B. E., & Franzreb, M. (2015). Optimization of enzyme immobilization on magnetic microparticles using 1-ethyl-3-(3-dimethylaminopropyl)carbodiimide (EDC) as a crosslinking agent. *Analytical Methods*, 7, 10291–10298.
- Klewicki, J. K., & Morgan, J. J. (1998). Kinetic behavior of Mn(III) complexes of pyrophosphate, EDTA, and citrate. *Environmental Science and Technology*, 32, 2916–2922.
- Kohl, P., & Medlar, S. (2006). *Occurrence of manganese in drinking water and manganese control*. USA: Awwa Research Foundation.
- Kujala, M., Sillanpää, M., & Rämö, J. (2004). A method to leach manganese and some other metal cations from pulp matrix to aqueous phase for the subsequent ICP-AES analysis: a potential tool for controlling the metal profile in a pulp bleaching process. *Journal of Cleaner Production*, 12, 707–712.
- Madison, A., Tebo, B., & Luther, G. W., III. (2011). Simultaneous determination of soluble manganese(III), manganese(II) and total manganese in natural (pore)waters. *Talanta*, 84, 374–381.
- Metsarinne, S., Ronkainen, E., Tuhkanen, T., Aksela, R., & Sillanpää, M. (2007). Biodegradation of novel amino acid derivatives suitable for complexing agents in pulp bleaching applications. *Science of the Total Environment*, 377, 45–51.
- Morhardt, C., Ketterer, B., Heißler, S., & Franzreb, M. (2014). Direct quantification of immobilized enzymes by means of FTIR ATR spectroscopy—a process analytics tool for biotransformations applying non-porous magnetic enzyme carriers. *Journal of Molecular Catalysis B:zymatic*, 107, 55–63.
- NS Energy (2020). Top five manganese ore mining countries across the globe. <https://www.nsenenergybusiness.com/features/manganese-producing-countries/>. Accessed 19 July 2020.
- Oviedo, C., & Rodríguez, J. (2003). EDTA: the chelating agent under environmental scrutiny. *Quimica Nova*, 26(6), 901–905.
- Pani, T., Das, A., Jabez, W., & Osborne, W. (2017). Bioremoval of zinc and manganese by bacterial biofilm: a bioreactor-based approach. *Journal of Photochemistry Photobiology B*, 175, 211–218.
- Pinto, I., Ascenso, O., Barros, M., & Soares, H. (2015). Pre-treatment of the paper pulp in the bleaching process using biodegradable chelating agents. *International Journal of Environmental Science and Technology*, 12, 975–983.
- Pinto, I., Neto, I., & Soares, H. (2013). Biodegradable chelating agents for industrial, domestic, and agricultural applications—a review. *Environmental Science and Pollution Research*, 12, 975–982.

- Roskill Metals and Minerals Reports (2019). Manganese: Outlook to 2029 (15th Edition). <https://roskill.com/market-report/manganese>. Accessed 19 July 2020.
- Schwabe, R., Anke, M. K., Szymańska, K., Wiche, O., & Tischler, D. (2018). Analysis of desferrioxamine-like siderophores and their capability to selectively bind metals and metalloids: Development of a robust analytical RP-HPLC method. *Research Microbiology*, *169*(10), 598–607.
- Sohn, S., & Kim, D. (2005). Modification of Langmuir isotherm in solution systems—definition and utilization of concentration dependent factor. *Chemosphere*, *58*, 115–123.
- Springer, S.D. & Butler, A. (2015). Magnetic susceptibility of Mn(III) complexes of hydroxamate siderophores. *Journal of Inorganic Biochemistry*, *148*, 22–26.
- Stengel, A., Gügel, I. L., Hilger, D., Rengstl, B., Jung, H., & Nickelsen, J. (2012). Initial steps of Photosystem II de Novo assembly and preloading with Manganese take place in Biogenesis Centers in Synechocystis. *The Plant Cell*, *24*, 660–675.
- Tanaka, N., Shirakashi, T., & Ogino, H. (1965). The oxidation-reduction potential of the system of Mn (II) EDTA-Mn (III) EDTA complexes and the stability constant of Mn (III) EDTA complex. *Bulletin of the Chemical Society of Japan*, *38*(9), 1515–1517.
- Thongpitak, J., Pekkoh, J., & Pumas, C. (2019). Remediation of Manganese-contaminated coal-mine water using bio-sorption and bio-oxidation by the Microalga *Pediastrum duplex* (AARLG060): a Laboratory-Scale Feasibility Study. *Front Microbiology*, *10*(2605), 1–14.
- Tian, H., Yuan, L., Wang, J., Wu, H., Wang, H., Xiang, A., et al. (2019). Electrospinning of polyvinyl alcohol into crosslinked nanofibers: an approach to fabricate functional adsorbent for heavy metals. *Journal of Hazardous Materials*, *378*, 120751.
- Tobiason, J., Bazilio, A., Goodwill, J., Mai, X., & Nguyen, C. (2016). Manganese removal from drinking water sources. *Current Pollution Report*, *2*, 168–177.
- Volpe, D. (2012) Assessment of Iron and Manganese Sequestration. Environmental & Water Resources Engineering Masters Projects, 53.
- Wang, Z. & Giammar, D.E. (2015). Metal Contaminant Oxidation Mediated by Manganese Redox Cycling in Subsurface Environment. Ch. 2. In Sparks, et al. (Eds.) *Advances in the Environmental Biogeochemistry of Manganese Oxides* (pp. 29–50). ACS Symposium Series; American Chemical Society: Washington, DC.
- Wilkesman, J., Mörtter, K., Sommer, I. & Kunz, P.M. (2019). Fishing manganese out from cellulose: impact of coupling desferrioxamine B to stainless steel beads on the circular economy of paper and pulp industry. AVS 66th International Symposium and Exhibition.
- Wright, M. H., Farooqui, S. M., White, A. R., & Greene, A. C. (2016). Production of manganese oxide nanoparticles by *Shewanella* species. *Applied and Environmental Microbiology*, *82*, 5402–5409.
- Ye, Z., Jeong, E., Wu, X., Tan, M., Yin, S., & Lu, Z. (2012). Polydisulfide Manganese(II) complexes as non-Gadolinium biodegradable macromolecular MRI contrast agents. *Journal of Magnetic Resonance Imaging*, *35*, 737–744.
- Zeiner, M., Rezić, T., Santek, B., Rezić, I., Hann, S. & Stinger, G. (2012). Removal of Cr, Mn, and Co from textile wastewater by horizontal rotating tubular bioreactor. *Environmental Science and Technology*, *46*, 10690–10696.
- Zhang, H., Herman, J. P., Bolton, H., Jr., Zhang, Z., Clark, S., & Xun, L. (2007). Evidence that bacterial ABC-type transporter imports free EDTA for metabolism. *Journal of Bacteriology*, *189*(22), 7991–7997.
- Zittel, W. (2012). Futures for the common good. Energy transition. Paths in a period of increasing scarcity. Ludwig-Bölkow-Systemtechnik. pp 1–83. https://www.umweltbuero.at/feasiblefutures/wp-content/uploads/Progress%2520Report%25201_Feasible%2520Futures_Zittel_final_14032012_WZ.pdf. Accessed 19 July 2020.

Affiliations

Peter M. Kunz¹ · **Kerstin Mörtter**¹  · **Ralf Müller**² · **Isabell Sommer**¹  ·
Philipp Weller²  · **Jeff Wilkesman**^{1,3} 

- ¹ Faculty of Process and Chemical Engineering, Institute for Biological Process Engineering, Mannheim University of Applied Sciences, Paul-Wittsack-Straße 10, D-68163 Mannheim, Germany
- ² Faculty of Biotechnology, Competency Center for Chemometrics CHARISMA, Institute for Instrumental Analysis and Bioanalytics, Mannheim University of Applied Sciences, Paul-Wittsack-Straße 10, D-68163 Mannheim, Germany
- ³ Centre for Environmental, Biology and Chemistry Research, Ambioquim, FACYT, Universidad de Carabobo, Valencia, Venezuela